Near-infrared image guidance in cancer surgery

Schaafsma, B.E.

Chapter 7

Near-infrared fluorescence-guided resection of colorectal liver metastases

Schaafsma BE[1], Van der Vorst JR[1], Hutteman M, Verbeek FPR, Liefers GJ, Hartgrink HH, Smit VTHBM, Löwik CWGM, van de Velde CJH, Frangioni JV, Vahrmeijer AL

[1] Shared first authorship

Cancer 2013;119:3411-3418

ABSTRACT

Background

The fundamental principle of oncologic surgery is the complete resection of malignant cells. However, small tumours are often difficult to find during surgery using conventional techniques. The objectives of this study were to determine if optical imaging, using a contrast agent already approved for other indications, could improve hepatic metastasectomy with curative intent, to optimize dose and timing, and to determine the mechanism of contrast agent accumulation.

Methods

The high tissue penetration of near-infrared (NIR) light was exploited by use of the FLARE (Fluorescence-Assisted Resection and Exploration) image-guided surgery system and the NIR fluorophore indocyanine green in a clinical trial of 40 patients undergoing hepatic resection for colorectal cancer metastases.

Results

A total of 71 superficially located (<6.2 mm beneath the liver capsule) colorectal liver metastases were identified and resected using NIR fluorescence imaging. Median tumour-to-liver ratio was 7.0 (range, 1.9 18.7) and no significant differences between time points or doses were found. Indocyanine green fluorescence was seen as a rim around the tumour, which is shown to be entrapment around cytokeratin 7 positive hepatocytes compressed by the tumour. Importantly, in 5 of 40 patients (12.5%, 95% confidence interval 55.0-26.6), additional small and superficially located lesions were detected using NIR fluorescence, and were otherwise undetectable by preoperative computed tomography, intraoperative ultrasound, visual inspection, and palpation.

Conclusions

NIR fluorescence imaging, even when used with a nontargeted, clinically available NIR fluorophore, is complementary to conventional imaging and able to identify missed lesions by other modalities.

INTRODUCTION

Prognosis and survival of patients with colorectal cancer depends primarily on the occurrence of distant metastases, which occur most frequently in the liver.[1] A resection with curative intent can offer patients with colorectal liver metastases a 5-year survival rate of 36% to 60%.[2-5] Despite improvements in preoperative imaging modalities, surgical techniques, and chemotherapy regimens, intrahepatic recurrence rates vary from 11% to 37.5% after hepatic metastasectomy, and 65% to 85% of these recurrences appear within 2 years after resection.[2,6-9] A possible explanation for this high intrahepatic recurrence rate is that some hepatic metastases are already present at the time of liver resection, but were undetected by the technology typically available in the community setting, namely, preoperative imaging, intraoperative ultrasound (IOUS), and inspection/palpation by the surgeon. For example, it is known that small and superficially located liver metastases are difficult to identify using available imaging modalities such as preoperative computed tomography (CT), magnetic resonance imaging (MRI), and IOUS.[10-12]

Near-infrared (NIR) fluorescence imaging using indocyanine green (ICG) is a promising technique to intraoperatively visualize the contrast between liver metastases and normal liver tissue in real time.[13-15] This type of optical imaging is relatively inexpensive and is quickly becoming widely available. Unlike visible light, which is used to excite fluorophores such as fluorescein, NIR light can penetrate several millimeters into tissue and through blood. ICG is excreted exclusively into the bile after intravenous injection; it has been hypothesized that colorectal liver metastases can be visualized due to passive accumulation of ICG caused by hampered biliary excretion, which results in a fluorescent rim around the metastases. However, the mechanism of ICG accumulation has not yet been explored.

Recently, Ishizawa et al[13] described the intraoperative detection of colorectal liver metastasis using NIR fluorescence imaging after intravenous injection of 0.5 mg/kg ICG, 1 to 14 days prior to surgery, as part of an ICG retention liver function test. The dose and interval between ICG injection and surgery are key determinants of the remaining background fluorescence signal in the liver and the fluorescent rim surrounding the tumour. In a preclinical study in rats performed by our group, the influence of injection time prior to surgery and dose of ICG pertaining to the contrast between the fluorescent rim around the hepatic metastases and normal liver tissue (tumour-to-liver ratio) was examined.[16] In this preclinical study, the highest tumour-to-liver ratio (TLR) was reached when ICG was injected 72 hours prior to surgery. Furthermore, this study demonstrated that even small liver metastases (≈1 mm in size) could be identified using NIR fluorescence. In this study, these preclinical results were translated to a clinical trial in patients with colorectal liver metastases in order to optimize intraoperative identification of liver metastases by using ICG. Furthermore, the mechanism of ICG accumulation in the transition area between tumour and

normal liver tissue was investigated, and the value added by NIR fluorescence imaging was determined.

MATERIALS AND METHODS

Preparation and Administration of ICG

ICG (25 mg vials) was purchased from Pulsion Medical Systems (Munich, Germany) and resuspended in 10 mL of sterile water for injection to yield a stock solution of 2.5 mg/mL (3.2 mM). Of this stock solution, 4 or 8 mL, corresponding to doses of 10 or 20 mg, were administered intravenously.

Clinical Trial

The study was approved by the Local Medical Ethics Committee of the Leiden University Medical Center, Leiden, The Netherlands, and was performed in accordance with the ethical standards of the Helsinki Declaration of 1975. All patients were evaluated for hepatic treatment by a multidisciplinary specialized liver unit (surgeon, oncologist, interventional radiologist, and an experienced abdominal radiologist). From 2010 to 2012, a total of 40 patients with suspected colorectal liver metastases, based on a preoperative 4-phase CT scan (Aquilion 64; Toshiba, Tokyo, Japan) of the thorax and abdomen with a slice thickness of 5 mm, who were planned to undergo curative-intended liver resection, were included. All patients provided informed consent. Exclusion criteria were pregnancy, lactation, or an allergy to iodine, shellfish, or ICG.

Patients received 10 or 20 mg of ICG diluted in a total volume of 4 and 8 mL, respectively, as an intravenous bolus at 24 or 48 hours prior to surgery on an inpatient basis. This resulted in 4 groups of 4 patients per group (N=16 patients). Subsequently, 24 patients were included at the optimal combination of ICG dose and injection time. After mobilization of the liver, first visual inspection, palpation, and IOUS were performed to determine the number and location of the liver metastases. To evaluate the additional benefit of NIR fluorescence imaging, all liver segments were imaged using the Mini-FLARE imaging system, which has been described.[17] Directly following liver resection, resection specimens were delivered to the Department of Pathology, where the specimens were sliced into 5- to 7-mm-thick slices and examined by an experienced pathologist for NIR fluorescence, using the Mini-FLARE imaging system.

Table 1. Study Subject Characteristics (N=40)

Characteristic	Median [Range] or (%)
Age	63 [45 - 77]
BMI	25 [19 - 38]
Sex	Male: 21 (52.5%) Female: 19 (47.5%)
Primary tumour location	
Colon	21 (52.5%)
Sigmoid	5 (12.5%)
Rectum	13 (32.5%)
Anus	1 (2.5%)
Neo-adjuvant chemotherapy	22 (55.0%)
Type of resection	
Hemihepatectomy	6 (15.0%)
Metastasectomy / segmentectomy	19 (47.5%)
Metastasectomy / segmentectomy + RFA	7 (17.5%)
RFA only	1 (2.5%)
No resection	7 (17.5%)

Abbreviations: BMI: body mass index; RFA: radiofrequency ablation.

Fluorescence Microscopy

On the basis of macroscopic evaluation and ex vivo fluorescence imaging, tissue was acquired from the transition zone between the tumour and the normal liver from multiple patients. Excised tissue was snap-frozen and sectioned at 5 lm for fluorescence and regular microscopy. Sections were measured for fluorescence using the Nuance multispectral imager (CRi, Woburn, Mass) mounted on a Leica DM IRE2 inverted microscope (Leica, Wetzlar, Germany). Subsequently, these slides were stained with hematoxylin and eosin. Consecutive slides were stained for the presence of CD31 (M0823; Dako, Glostrup, Denmark), CK7 (M7018; Dako), and CD68 (M0814; Dako) to correlate fluorescence to blood vessels, bile ducts, and macrophages, respectively. White light images were subsequently merged with fluorescence images.

Statistical Analysis

For statistical analysis, the SPSS version 17.0 statistical software package (SPSS, Chicago, Ill) was used. TLR signal, rim fluorescence, and background fluorescence were reported as median and range. Tumour size was reported as mean with standard deviation. To test differences between groups, the Kruskal-Wallis 1-way analysis of variance test was used to test for differences between time and dose groups. Statistical tests were 2-tailed, and $P<.05$ was considered significant. The 95% binomial confidence intervals (CIs) of the percentage of patients in whom additional metastases were identified were calculated using the adjusted Wald method by GraphPad QuickCalcs (Graph- Pad Software, La Jolla, Calif).

Table 2. Methods of detection

Modality	Number of hepatic metastases identified*(%)	Number of patients	Size of metastases (mm)
Preoperative CT-scan	73 (75)	39	29.9 ± 19.1
IOUS, palpation and inspection	92 (95)	40	26.3 ± 19.5
NIR fluorescence	71 (73)	37	29.0 ± 29.8
Preoperative CT-scan, IOUS, inspection palpation and/or NIR fluorescence	97 (100)	40	24.5 ± 19.7

*Liver metastases were confirmed by histology or in the case of nonresected lesions by clinical appearance, IOUS, and CT.

RESULTS

Study Subjects

Patient and tumour characteristics of the 40 patients are listed in Table 1. None of the patients suffered from hepatitis or liver cirrhosis, and 22 patients received neoadjuvant chemotherapy. In 7 patients, no liver resection was performed due to invasion of tumour into the portal vein (N=3), the presence of additional unresectable liver metastases (N=2), or the appearance of lymph node metastases (N=2). Nevertheless, these patients were included for TLR, rim fluorescence, and background fluorescence analysis.

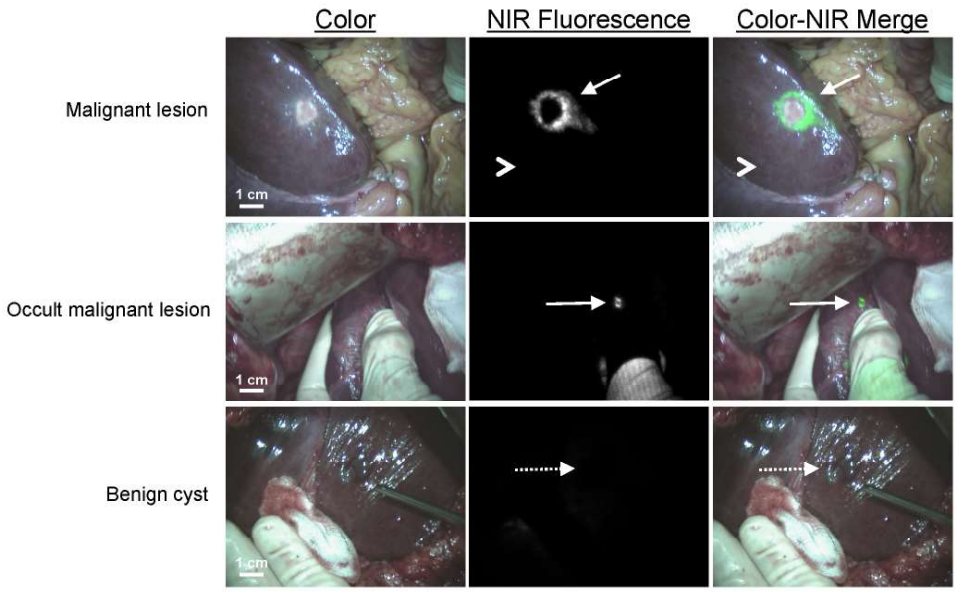

Fig. 1. Near-infrared (NIR) fluorescence imaging of colorectal liver metastases is shown. A colorectal liver metastasis (arrow) is clearly identified by a rim around the tumour in vivo (top row), 24 hours after injection of 10 mg indocyanine green. Normal liver tissue (arrowhead) shows minimal background uptake of indocyanine green. In 5 patients, small, superficial, otherwise occult metastases (middle row, arrow) were identified by NIR fluorescence imaging. Benign lesions (bottom row, dashed arrow) could be differentiated from malignant lesions by a lack of a fluorescent rim around the lesion.

Optimization of ICG Dose and Injection Timing (N=16 Patients)

To determine the effect of ICG dosage and postinjection imaging time, patients were allocated to 2 dose groups and imaged at 2 time points after ICG administration, resulting in 4 groups containing 4 patients per group. Fluorescence intensity of the rim around the liver metastases was significantly higher than the fluorescent signal in the liver (P<.001). Median TLR in all 16 patients was 7.3 (range, 1.9-18.7). Median TLRs were 5.0 (range, 2.2-15.4), 6.7 (range, 2.7-9.2), 10.5 (range, 1.9-18.7), 8.0 (range, 7.0-9.3) for the patient groups of 10 mg at 24 hours, 20 mg at 24 hours, 10 mg at 48 hours, and 20 mg at 48 hours, respectively. Median rim fluorescence (normalized pixel value) was 530.1 (range, 257.89-823.0), 938.4 (range, 902.3-1239.1), 648.6 (range, 137.1-1929.36), and 608.5 (range, 507.6-688.1) for the patient groups of 10 mg at 24 hours, 20 mg at 24 hours, 10 mg at 48 hours, and 20 mg at 48 hours, respectively. Median background fluorescence (normalized pixel value) was 98.3 (range, 53.6-127.6), 209.1 (range, 96.1-356.5), 64.6 (range, 53.4-112.4), and 77.4 (range, 67.5-96.2) for the patient groups of 10 mg at 24 hours, 20 mg at 24 hours, 10 mg at 48 hours, and 20 mg at 48 hours, respectively. Using the independent samples Kruskal Wallis test, no significant differences in signal-to-background ratios (P=.70), rim fluorescence (P=.67), and background fluorescence were observed (P=.08). Because no differences in TLRs were observed between the various groups, the optimal dose was determined by clinical and logistical preferences (the minimal dose of 10 mg of ICG administered 24 hours prior to surgery).

Intraoperative Detection of Colorectal Liver Metastases (N=40 Patients)

Subsequently, 24 more patients were included to assess the added value of NIR fluorescence imaging during resection of colorectal liver metastases. Results of liver metastases detection are summarized in Table 2. Using a combination of preoperative CT scanning, IOUS, visual inspection, and/or palpation, a total of 100 lesions were identified as suspected colorectal liver metastases. After resection, 3 of these lesions were histologically proven to be benign, for a net detection of 97 metastatic lesions by conventional imaging. NIR fluorescence imaging (Fig. 1 and Supplementary Video) detected a total of 71 lesions proven histologically to be metastases, all of which were ≤ 6.2 mm from the surface of the liver capsule. However, only 66 of the 71 lesions identified using NIR fluorescence overlapped with conventional imaging (Table 2 and Fig. 2). Most important, in 5 patients (12.5%, 95%CI = 5.0-26.6), superficially located, otherwise occult liver metastases were detected using NIR fluorescence only, but not by conventional imaging (ie, preoperative CT, IOUS, intraoperative visualization, and intraoperative palpation) (Fig. 1). Sensitivity of the preoperative CT scanning, intraoperative visual inspection/palpation in combination with IOUS, and

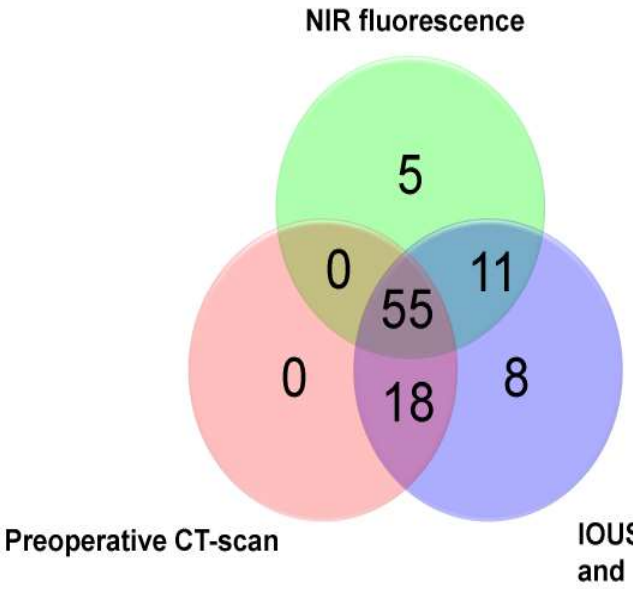

Fig. 2. Methods of detection of colorectal liver metastases are shown. Venn diagram shows how the 97 hepatic metastases were detected as a function of each modality alone or in combination. Abbreviations: CT, computed tomography; IOUS, intraoperative ultrasound; NIR, near infrared.

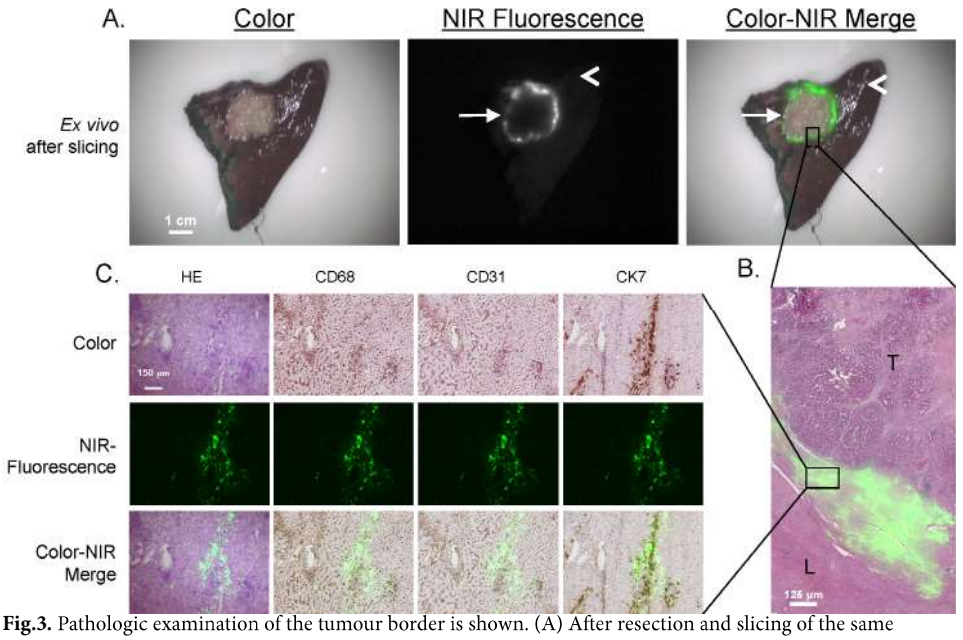

Fig.3. Pathologic examination of the tumour border is shown. (A) After resection and slicing of the same specimen, the rim around the tumour (arrow) can be visualized ex vivo. (B) Shown are hematoxylin and eosin (HE) staining with a pseudocolored green near-infrared (NIR) fluorescence overlay of a 20 lm tissue section of a colorectal liver metastasis using a 53 objective. The fluorescent rim in stromal tissue appears in the transition zone between tumour (T) and normal liver tissue (L). (C) Shown is liver tissue located in the fluorescent rim of a colorectal liver metastasis. Consecutive frozen sections (5 lm) are stained with HE and for CD68, CD31, and CK7. Microscopic color images (left column), NIR fluorescence images (middle column), and a pseudocolored green merge (right column) were obtained (1003 zoom). The NIR fluorescence signal is mainly located intracellularly and shows a high correlation with CK7 staining.

NIR fluorescence imaging were 75%, 95%, and 73%, respectively. In 3 patients, an additional wedge resection was performed to resect these metastases, and in 2 patients, the preoperatively planned metastasectomy was extended to resect the additional metastases. In these 5 patients, the total number of metastases (including the occult metastases detected only by NIR fluorescence) were 4, 3, 3, 2, and 2. After resection, these lesions were found to be 2, 3, 4, 6, and 9 mm in diameter, and histopathological examination confirmed these lesions to be colorectal liver metastases. One of these 5 occult lesions, which was 9 mm in diameter, was labeled as a complicated cyst based on IOUS and CT, whereas the clear NIR fluorescent ring around the lesion suggested that it was a liver metastasis. Twenty-six liver metastases (27%) identified by conventional imaging could not be detected using NIR fluorescence, and all were deeper than 8 mm from the liver surface. All fluorescent liver metastases presented a fluorescent rim around the tumour. The overall (N=40) median TLR was 7.0 (range, 1.9-18.7). The use of neoadjuvant chemotherapy did not significantly influence the TLR (7.5±5.1 versus 7.1±2.9, P=.77). In addition to liver metastases, a total of 8 hemangiomas, 13 cysts, and 4 bile duct hamartomas were identified in 13 patients. These hemangiomas, cysts, and bile duct hamartomas did not show an NIR fluorescent signal or rim (Fig. 1). Thus, NIR fluorescence imaging might help differentiate malignant liver lesions from some benign lesions. As might be expected based on the mechanism of ICG contrast (described below), extrahepatic tumour-positive lymph nodes were not fluorescent (data not shown).

Ex Vivo Detection of Colorectal Liver Metastases

Liver resection specimens were sliced into 5- to 7-mm slices, and subsequently the slices were imaged with the Mini-FLARE imaging system. In all patients for whom a liver resection was performed (N=33), ex vivo NIR fluorescence imaging was performed. All known metastases were identified ex vivo by a clear fluorescent ring around the lesion.

Immunohistochemistry and Fluorescence Microscopy

Fluorescence signal was located in liver tissue directly surrounding the tumour and was located both intracellularly and extracellularly (Fig. 3B). In liver tissue, in the area near the tumour, compressed hepatocytes and increased ductular transformation, periportal fibrosis, and presence of Kupffer cells were observed. Immunohistochemical analysis showed a close relation between fluorescence and CK7 staining (Fig. 3C). CK7 is expressed by immature hepatocytes in the areas of ductular transformation. No relation was found between fluorescence and the presence of Kupffer cells (CD68) and blood vessels (CD31).

DISCUSSION

The main objective of this study was to evaluate the potential of intraoperative NIR fluorescence imaging to improve oncologic resection of colorectal metastases to liver. As confirmed by pathological analysis, all superficially located (<6.2 mm beneath the liver surface) metastases were identified by NIR fluorescence. In addition, in 5 patients, occult metastases were detected using NIR fluorescence only and were missed by conventional detection methods (Fig. 2). Moreover, this study provides increased understanding of the mechanism responsible for the rim fluorescence and increases the understanding of the effect of different administration time points and doses of ICG on tumour detection. This is crucial for the implementation of this technique and interpretation of results in future studies.

An important recent study using visible wavelength optical imaging showed real-time identification of ovarian cancer metastases.[18] Because of the relatively low tissue penetration of visible light, this technology is limited to tumours already on the surface of anatomical structures. Even when NIR fluorescence imaging is used, however, penetration depth is still a major issue. The penetration depth of NIR light is highly dependent on the optical properties, ie, absorption and scatter, of the tissue being imaged. Liver is highly absorbing compared with other tissues, such as breast and subcutaneous tissue of axilla, resulting in higher attenuation (ie, lower signal).[19] In the current study, 26 metastases that were located 8 mm or more beneath the liver capsule could not be identified using NIR fluorescence. Preoperative CT scanning and IOUS are more appropriate for deeper lesions and did successfully identify these 26 lesions. However, superficially located, small occult metastases are known to be difficult to detect using IOUS, inspection, and palpation.[10,11] Although IOUS is still required to identify deep (≥6 mm) metastases in the liver, our results suggest that NIR fluorescence imaging is complementary and helps to find small, superficially located liver metastases.

The use of NIR fluorescence imaging to detect liver metastases is dependent on the clearance of ICG by the liver. To optimize the use of this technique, it is necessary to examine the influence of ICG dose and timing of ICG administration prior to surgery. In this study, differences in dose and timing did not significantly influence the TLR. A previous study in rats by our group showed an optimal TLR in the group where ICG was administered at 72 hours prior to surgery.[16] In the current clinical study, liver signal at 24 to 48 hours after injection of 10 mg ICG was comparable to the preinjection baseline level, which we measured in a previous study in patients undergoing a pancreatoduodenectomy, eliminating the need to test other time points.[20] Therefore, NIR fluorescence imaging at 72 hours after ICG administration was not performed. Other clinical work performed by Ishizawa et al suggested an interval between administration of ICG and liver surgery of at least 2 days to lower

background fluorescence and to obtain adequate TLRs.[13] However, in the latter study, a substantially higher dose of ICG (0.5 mg/kg; ≈35 mg per subject) was administered. In the current study, a relatively low dose of ICG (0.13-0.26 mg/ kg) was used, and it was therefore possible to reach acceptable TLRs and sufficiently low background liver fluorescence at 24 hours after administration of 10 mg ICG, which is safe and desirable from a logistical point of view.

Because no clinical data on lesion detection rates and standard deviation of the measurements were available prior to the study, a formal sample size calculation was not possible. However, we have provided 95% CIs for the 12.5% of patients in which additional lesions were detected only by NIR fluorescence (95%CI = 5.0-26.6). Well-powered future studies can now be designed on the basis of these data.

The detection rate of additional occult liver metastases during surgery is strongly dependent on the preoperative and intraoperative imaging modalities used. In this study, preoperative CT and IOUS were acquired to assess the extent of the disease. However, multiple novel imaging instruments are available for improved preoperative and intraoperative assessment of occult liver metastases. MRI benefits from increased soft tissue contrast and the availability of hepatocyte-specific contrast agents, which yields a higher sensitivity compared with CT for the detection of subcentimeter liver metastases and in case of neoadjuvant chemotherapy.[21,22] Moreover, [18F] fluorodeoxyglucose positron emission tomography (FDG-PET) or PET-CT has been shown to be of additional value to detect extrahepatic disease.[21] However, the sensitivity of detection of occult liver metastases using PET is not higher than that of CT.[21] Despite the possible higher detection rate using MRI, it can be expected that lesions missed during preoperative imaging could be detected during IOUS or palpation, which will therefore not significantly alter the finding of the current study. Next to preoperative imaging modalities, novel modalities for intraoperative assessment of occult liver metastases, such as contrast-enhanced IOUS, have been introduced to improve sensitivity.[23,24] However, NIR fluorescence has been shown to add value when used in combination with contrast-enhanced IOUS as well.[23]

An important aspect of our study is that it can be readily translated to the community setting. First, it uses a contrast agent already approved by the US Food and Drug Administration for other indications. Second, multiple optical imaging systems are now available commercially and are comparable in size, cost, and upkeep to an IOUS instrument. Finally, unlike PET, MRI, and other emerging imaging technologies that require significant infrastructure investment and high operational costs, cart-based optical imaging is potentially viable in any clinical setting.

Although the false-positive rate in the current study was zero, previous studies have reported that nonmalignant lesions (large regenerative nodules and atypical hyperplastic nodules) display ICG uptake.[13,14] The pattern of uptake appears to be important. In large regenerative nodules and atypical hyperplastic nodules, NIR

fluorescence is seen throughout the tumour (versus only in the rim). In the benign lesions (hemangiomas, cysts, and bile duct hamartomas) of our study, no fluorescence rim was seen. Clearly, larger clinical trials will be needed to determine the true false-positive rate and pattern of uptake of ICG as a function of benign lesion histology.

Using fluorescence microscopy, we observed intracellular accumulation of ICG in and around CK7-positive cells directly surrounding the tumour, and being compressed by it. The architecture of the liver parenchyma is often changed by the presence of hepatic metastases leading to compression of hepatic parenchyma, inflammatory infiltrate, ductular transformation, and increased presence of immature hepatocytes.[25-27] It is known that immature hepatocytes often have impaired expression of their organic anion transporters, which are essential for the transport of many organic anions, including ICG.[28-32] For example, in the absence of multidrug resistance P-glycoprotein 2, the biliary excretion of ICG can be reduced by 90%.[33] Therefore, the pattern of rim fluorescence could be explained by the presence of immature hepatocytes in the liver tissue surrounding the tumour that have taken up ICG, but exhibit impaired biliary clearance.

As in other areas of surgery, the use of laparoscopy is expanding to liver surgery. Minor liver resections such as left lateral hepatectomies are being performed laparoscopically as standard-of-care in several centers.[34] NIR fluorescence may also be of great value in laparoscopic surgery, because palpation of the liver is not possible and the surgeon can only rely on visual inspection, IOUS, and preoperative imaging. To implement NIR fluorescence in laparoscopic liver surgery, laparoscopic NIR fluorescence camera systems are currently being developed and tested.[35-37]

In conclusion, this study demonstrates identification of otherwise undetectable cancer metastases in 12.5% of patients and suggests that intraoperative NIR fluorescence imaging is complementary to conventional techniques for the detection of liver metastases from colorectal cancer, and has great potential for laparoscopic procedures

ACKNOWLEDGMENTS

This study was performed within the framework of CTMM, the Center for Translational Molecular Medicine (DeCoDe project, grant 03O-101 and MUSIS project, grant 03O-202). This work was supported in part by the Gastrostart grant (Dutch Association for Gastroenterology), the Dutch Cancer Society grant UL2010-4732 and National Institutes of Health grant R01-CA-115296. Dr. van der Vorst is an MD medical research trainee funded by the Netherlands Organisation for Health Research and Development (grant 92003593).

REFERENCES

1. Manfredi S, Lepage C, Hatem C, et al. Epidemiology and management of liver metastases from colorectal cancer. Ann Surg. 2006;244:254-259.
2. Abdalla EK, Vauthey JN, Ellis LM, et al. Recurrence and outcomes following hepatic resection, radiofrequency ablation, and combined resection/ablation for colorectal liver metastases. Ann Surg. 2004;239:818-825.
3. Choti MA, Sitzmann JV, Tiburi MF, et al. Trends in long-term survival following liver resection for hepatic colorectal metastases. Ann Surg. 2002;235:759-766.
4. Pawlik TM, Izzo F, Cohen DS, et al. Combined resection and radiofrequency ablation for advanced hepatic malignancies: results in 172 patients. Ann Surg Oncol. 2003;10:1059-1069.
5. Rees M, Tekkis PP, Welsh FK, et al. Evaluation of long-term survival after hepatic resection for metastatic colorectal cancer: a multifactorial model of 929 patients. Ann Surg. 2008;247: 125-135.
6. Wei AC, Greig PD, Grant D, et al. Survival after hepatic resection for colorectal metastases: a 10-year experience. Ann Surg Oncol. 2006;13:668-676.
7. Pawlik TM, Scoggins CR, Zorzi D, et al. Effect of surgical margin status on survival and site of recurrence after hepatic resection for colorectal metastases. Ann Surg. 2005;241:715-722.
8. Karanjia ND, Lordan JT, Fawcett WJ, et al. Survival and recurrence after neo-adjuvant chemotherapy and liver resection for colorectal metastases: a ten year study. Eur J Surg Oncol. 2009;35:838-843.
9. Fong Y, Cohen AM, Fortner JG, et al. Liver resection for colorectal metastases. J Clin Oncol. 1997;15:938-946.
10. Leen E, Ceccotti P, Moug SJ, et al. Potential value of contrastenhanced intraoperative ultrasonography during partial hepatectomy for metastases: an essential investigation before resection? Ann Surg. 2006;243:236-240.
11. Sahani DV, Kalva SP, Tanabe KK, et al. Intraoperative US in patients undergoing surgery for liver neoplasms: comparison with MR imaging. Radiology. 2004;232:810-814.
12. Nomura K, Kadoya M, Ueda K, et al. Detection of hepatic metastases from colorectal carcinoma: comparison of histopathologic features of anatomically resected liver with results of preoperative imaging. J Clin Gastroenterol. 2007;41:789- 795.
13. Ishizawa T, Fukushima N, Shibahara J, et al. Real-time identification of liver cancers by using indocyanine green fluorescent imaging. Cancer. 2009;115:2491-2504.
14. Gotoh K, Yamada T, Ishikawa O, et al. A novel image-guided surgery of hepatocellular carcinoma by indocyanine green fluorescence imaging navigation. J Surg Oncol. 2009;100:75-79.
15. Verbeek FP, van der Vorst JR, Schaafsma BE, et al. Image-guided hepatopancreatobiliary surgery using near-infrared fluorescent light. J Hepatobiliary Pancreat Sci. 2012;19:626-637.
16. van der Vorst JR, Hutteman M, Mieog JS, et al. Near-infrared fluorescence imaging of liver metastases in rats using indocyanine green. J Surg Res. 2012;174:266-271.
17. Mieog JS, Troyan SL, Hutteman M, et al. Toward optimization of imaging system and lymphatic tracer for near-infrared fluorescent sentinel lymph node mapping in breast cancer. Ann Surg Oncol. 2011;18:2483-2491.
18. van Dam GM, Themelis G, Crane LM, et al. Intraoperative tumorspecific fluorescence imaging in ovarian cancer by folate receptoralpha targeting: first in-human results. Nat Med. 2011;17:1315- 1319.
19. Stolik S, Delgado JA, Perez A, et al. Measurement of the penetration depths of red and near infrared light in human "ex vivo" tissues. J Photochem Photobiol B. 2000;57:90-93.
20. Hutteman M, van der Vorst JR, Mieog JS, et al. Near-infrared fluorescence imaging in patients undergoing pancreaticoduodenectomy. Eur Surg Res. 2011;47:90-97.
21. Frankel TL, Gian RK, Jarnagin WR. Preoperative imaging for hepatic resection of colorectal cancer metastasis. J Gastrointest Oncol. 2012;3:11-18.
22. van Kessel CS, Buckens CF, van den Bosch MA, et al. Preoperative imaging of colorectal liver metastases after neoadjuvant chemotherapy: a meta-analysis. Ann Surg Oncol. 2012;19:2805-2813.

23. Uchiyama K, Ueno M, Ozawa S, et al. Combined use of contrast-enhanced intraoperative ultrasonography and a fluorescence navigation system for identifying hepatic metastases. World J Surg. 2010;34:2953-2959.
24. Takahashi M, Hasegawa K, Arita J, et al. Contrast-enhanced intraoperative ultrasonography using perfluorobutane microbubbles for the enumeration of colorectal liver metastases. Br J Surg. 2012;99:1271-1277.
25. Irie T, Tsushima Y, Terahata S, et al. Rim enhancement in colorectal metastases at CT during infusion hepatic arteriography. Does it represent liver parenchyma or live tumor cell zone? Acta Radiol. 1997;38:416-421.
26. Marchal GJ, Pylyser K, Tshibwabwa-Tumba EA, et al. Anechoic halo in solid liver tumors: sonographic, microangiographic, and histologic correlation. Radiology. 1985;156:479-483.
27. Vermeulen PB, Colpaert C, Salgado R, et al. Liver metastases from colorectal adenocarcinomas grow in three patterns with different angiogenesis and desmoplasia. J Pathol. 2001;195:336-342.
28. Oshima H, Kon J, Ooe H, et al. Functional expression of organic anion transporters in hepatic organoids reconstructed by rat small hepatocytes. J Cell Biochem. 2008;104:68-81.
29. de Graaf W, H€ausler S, Heger M, et al. Transporters involved in the hepatic uptake of (99m) Tc-mebrofenin and indocyanine green. J Hepatol. 2011;54:738-745.
30. Cui Y, Konig J, Leier I, et al. Hepatic uptake of bilirubin and its conjugates by the human organic anion transporter SLC21A6. J Biol Chem. 2001;276:9626-9630.
31. Yang YM, Tian XD, Zhuang Y, et al. Risk factors of pancreatic leakage after pancreaticoduodenectomy. World J Gastroenterol. 2005;11:2456-2461.
32. Ros JE, Roskams TA, Geuken M, et al. ATP binding cassette transporter gene expression in rat liver progenitor cells. Gut. 2003;52: 1060-1067.
33. Huang L, Vore M. Multidrug resistance p-glycoprotein 2 is essential for the biliary excretion of indocyanine green. Drug Metab Dispos. 2001;29:634-637.
34. Chang S, Laurent A, Tayar C, et al. Laparoscopy as a routine approach for left lateral sectionectomy. Br J Surg. 2007;94:58-63.
35. Matsui A, Tanaka E, Choi HS, et al. Real-time intra-operative near-infrared fluorescence identification of the extrahepatic bile ducts using clinically available contrast agents. Surgery. 2010;148:87-95.
36. van der Poel HG, Buckle T, Brouwer OR, et al. Intraoperative laparoscopic fluorescence guidance to the sentinel lymph node in prostate cancer patients: clinical proof of concept of an integrated functional imaging approach using a multimodal tracer. Eur Urol. 2011;60:826-833.
37. Ishizawa T, Bandai Y, Kokudo N. Fluorescent cholangiography using indocyanine green for laparoscopic cholecystectomy: an initial experience. Arch Surg. 2009;144:381-382.